YIFAN SUN[1]
E-mail: m18705423520@163.com
JINGLEI ZHANG[1]
(Corresponding author)
E-mail: jinglei@sdut.edu.cn
XIAOYUAN WANG, Ph.D.[1]
E-mail: 2674289091@qq.com
ZHANGU WANG[1]
E-mail: 1348035225@qq.com
JIE YU[1]
E-mail:1206674681@qq.com
[1] School of Transportation and Vehicle Engineering
Shandong University of Technology
No. 12 Zhangzhou Road, Zhangdian District, Zibo City,
Shandong Province, China

Swarm Intelligence in Transportation Engineering
Original Scientific Paper
Submitted: 18 July 2017
Accepted: 5 Feb. 2018

RECOGNITION METHOD OF DRINKING-DRIVING BEHAVIORS BASED ON PCA AND RBF NEURAL NETWORK

ABSTRACT

Drinking-driving behaviors are important causes of road traffic injuries, which are serious threats to the lives and property of traffic participants. Therefore, reducing the occurrences of drinking-driving behaviors has become an important problem of traffic safety research. Forty-eight male drivers and six female drivers who could drink moderate alcohol were chosen as participants. The drivers' physiological data, operation behavior data, car running data, and driving environment data were collected by designing various virtual traffic scenes and organizing drivers to conduct driving simulation experiments. The original variables were analyzed by the Principal Component Analysis (PCA), and seven principal components were extracted as the input vector of the Radial Basis Function (RBF) neural network. The principal component data was used to train and verify the RBF neural network. The Levenberg-Marquardt (LM) algorithm was chosen to train the parameters of the neural network and build a drinking-driving recognition model based on PCA and RBF neural network to realize an accurate recognition of drinking-driving behaviors. The test results showed that the drinking-driving recognition model based on PCA and RBF neural network could identify drinking drivers accurately during driving process with a recognition accuracy of 92.01%, and the operation efficiency of the model was high. The research can provide useful reference for prevention and treatment of drinking and driving and traffic safety maintenance.

KEY WORDS

traffic safety; drinking-driving behaviors; recognition method; principal component analysis; radial basis function neural network;

1. INTRODUCTION

With the development of the automobile industry, the world's car ownership has risen sharply. Cars are convenient for people's livelihood, but they also bring serious traffic safety problems [1]. Statistics show that there were 104 production safety accidents in China during the period from January to February of 2016. Traffic accidents accounted for 61.54%, and the death toll percentage of traffic accidents was 58.61%, which was the highest death toll percentage among the various accidents [2]. Drinking and driving is an important factor which increases traffic accident death rates related to young adults [3]. Thus, it has been a key issue in the traffic safety field to take effective measures to reduce or eliminate drinking and driving.

Many countries, including the United States, the United Kingdom, and China, have fully realized the urgency of drinking-driving governance currently, and have taken various methods to prevent drinking-driving behaviors, such as legislation, carrying out publicity, and education. The key to drinking-driving governance is whether to identify drinking-driving behaviors accurately or not, and stop drinking and driving in time. The traditional passive drinking-driving recognition methods rely on traffic police and other law enforcement authorities to do alcohol tests by intercepting drivers. The passive drinking-driving recognition methods have not been adapted to current needs, because the number of cars has increased significantly. Thus, for drinking-driving prevention and traffic safety purposes, active drinking-driving recognition methods should be developed to identify drinking drivers automatically and accurately before or during the driving processes.

Some researchers studied several advanced active drinking-driving recognition methods based on different techniques. In 2007, the alcohol key technique was first used by Svenska Aeroplan Aktiebolaget (SAAB) [4]. A miniature alcohol detection device was placed in the car key, and drivers had to complete the alcohol test by blowing into the car key before

starting cars. However, the method was easily dismissed for failing to determine whether alcohol-based gases were exhaled by drivers or not. In 2009, YC Wu used cameras to capture driver's face images to compare them with images of driver's face in sober condition to determine whether the driver had been drinking or not [5]. However, this method was easily affected by environmental factors such as illumination, so its accuracy was poor. The driving state can be reflected by driving behaviors and continuity, and noninvasiveness of driving behavior data can provide new ideas on drinking-driving recognition methods. Therefore, drinking-driving recognition methods based on driving behaviors are an important aspect in studying active drinking-driving recognition methods [6-7]. In 2014, Xiaohua Z [8] obtained the data of drivers' subjective feelings and driving behaviors under different blood alcohol concentration (BAC) levels using a driving simulator. The characteristics of the drinking-driving behaviors and car motion were analyzed based on the experimental data. Relevant data on average speed, speed standard deviation, and lane line position was analyzed, whereby standard deviation changed observably after drinking. Whether the drivers were in the drinking-driving state or not could be detected based on changes of the three variables.

Driving behavior factors influencing the recognition of drinking and driving are various, and there are complex relationships among the various factors, so the nonlinear fitting capacity of the drinking-driving recognition model should be high. The RBF neural network [9-11] is an adaptive dynamic system that is interconnected by many neurons. It is a type of a multi-level neural network that converges faster. The non-linearity and high robustness of the RBF neural network makes it an effective tool for solving complex pattern recognition problems. However, the learning speed of the RBF neural network is strongly influenced by total input data, and PCA can reduce the amount of input data by reducing the dimensions of affected factors and the multi-collinearity between factors. Therefore, PCA and the RBF neural network model were used in this paper to achieve accurate recognition of drinking-driving behaviors. To simplify the RBF neural network and avoid long training and local minima, the LM algorithm [12-14] was used to train the neural network, rather than the gradient descent method.

In this paper, the information collection system for the driver's body, car, and the environment was used to gather the physiological data, operation behavior data, car running data, and driving environment data of drivers in human factor experiments and driving simulation experiments. Some variables influencing drinking-driving recognition were chosen to be analyzed by PCA, and a drinking-driving recognition model based on PCA and the RBF neural network was established for automatic identification of drinking-driving behaviors. It has shown that the model can fuse the information of driver's body, car, and the environment. In addition, it can recognize drinking-driving behaviors accurately and automatically at the same time during the driving process.

2. DRINKING-DRIVING RECOGNITION MODEL BASED ON PCA AND RBF NEURAL NETWORK

The design diagram of the drinking-driving recognition model based on PCA and RBF neural network is shown in *Figure 1*.

Many original variables can be converted to several uncorrelated principal components by PCA, and the major information of original variables can be preserved. Thus, PCA reduces the complexities of data analysis [15-16]. Multiple influencing variables of drinking-driving recognition were analyzed by PCA in order to improve the speed of network training. A vector consisting of obtained principal components was applied as the input vector of the RBF neural network. The PCA mathematical model is as follows:

$$Z = AV \tag{1}$$

$V=(v_1,v_2,...,v_p)$ is the vector consisting p of original variables, which are driver's body, car, and environment variables related to drinking-driving recognition. The data of $V=(v_1,v_2,...,v_p)$ are standardized data so the mean value is 0, and the standard deviation is 1. $Z=(z_1,z_2,...,z_i)$ consists of i principal components ($i<p$) and is the input vector of the RBF neural network; A is the principal component score coefficient matrix.

The RBF neural network includes three layers. The layers consist of neurons whose number is indefinite. The transformation function of hidden layer neurons is a radial basis function. The RBF neural network is the unity of the linear mapping and nonlinear mapping; the mappings between the input layer and hidden layer are nonlinear, and the mappings between the hidden layer and output layer are linear. Thus, the RBF neural network has the advantages of fast learning and overcoming local minima [17].

In *Figure 1*, the input vector $Z=(z_1,z_2,...,z_i)$ of the RBF neural network is the result of PCA, which contains the most of driving behavior information. There is one input layer, one hidden layer, and one output layer. The number of input layer neurons is i (the number of principal components). Considering the speed and accuracy of the training, the number of hidden layer neurons is designed to be 12. The radial basis function is used as the activation function of hidden layer neurons. The input vector is mapped to hidden space directly, rather than through the connection based on weight value. The Gaussian function was chosen as the radial basis function, and the function formula is as follows:

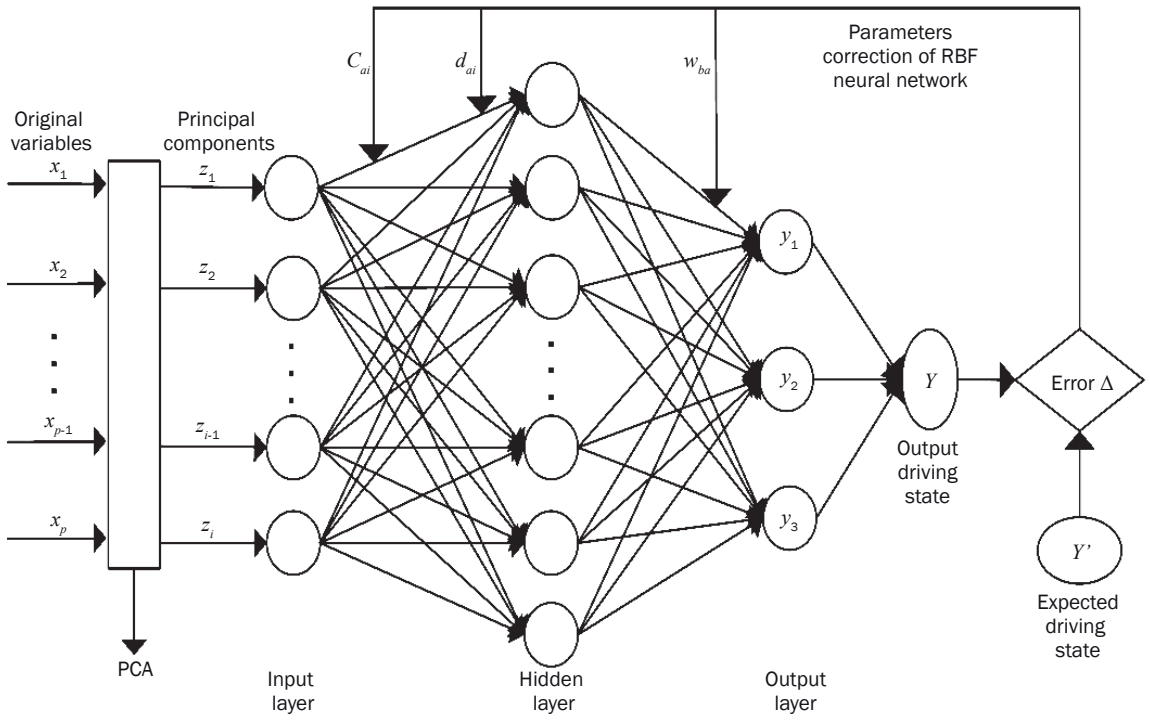

Figure 1 – Combination model framework of PCA and RBF neural network

$$\phi_a = g(\|Z - C_a\|) = \exp\left(-\frac{1}{2D_a}\|Z - C_a\|^2\right) \quad (2)$$

In *Formula 2*, ϕ_a is output value of hidden layer neurons (a); $g_{(x)}$ is Gaussian function; $\|\ldots\|$ is Euclidean norm; $Z=(z_1,z_2,\ldots,z_i)$ is input vector; $C_a=(c_{a1},c_{a2},\ldots,c_{ai})$ is the central parameter vector of the Gaussian function of hidden layer neurons (a); $D_a=(d_{a1},d_{a2},\ldots,d_{ai})$ is variance vector of the Gaussian function of hidden layer neurons (a).

There are three neurons in the output layer, which represent three types of driving states. Outcome $Y=y_j$ (j=1,2,3) is the output driving state value of the model, $Y'=y_j$ (j=1,2,3) is the expected driving state value, y_1=(1,1,1) represents the normal driving state, y_2=(0,0,1) represents the drinking-driving state (0.02%≤BAC≤0.08%), and y_3=(0,0,0) represents the drunk driving state (BAC≥0.08%). The mapping between hidden layer and output layer is linear, the output function of output layer neurons is as follows:

$$y_b = \sum_{a=1}^{12} w_{ba}\phi_a \quad (3)$$

In *Formula 3*, y_b is the output value of the output neuron b; w_{ba} is the connection weight between the output neuron b and hidden neuron a; ϕ_a is the output value of the hidden neuron a.

The sample data spread forward along the neural network and reach the output layer through the processes of all hidden neurons. In the end, three types of driving states can be obtained. The parameters of the RBF neural network are amended according to the method which can reduce the error between output driving state value and expected driving state value. The sample data is used to train the RBF neural network until the desired error is met, and the drinking-driving recognition model is established.

3. DATA ACQUISITION AND CHOICES OF VARIABLES

3.1 Acquisition of experimental data

Participants

Given that male drivers are more likely to be drunk driving than female drivers, and young drivers are more impulsive and take more risks than older drivers, we focused on young and male drivers. 54 drivers were selected as participants and numbered, 48 male drivers and 6 female drivers among them. Their average age was 27 years. The cumulative driving mileage was more than 50,000 kilometers, and the participants had driving experience and stable driving habits. All the participants were in good physical and mental condition, and they could drive manual cars masterly. They were able to handle alcohol and complete the experiments after drinking.

Experimental apparatus

The experimental apparatus is shown in *Figure 2*, including the human factors experimental apparatus for gathering drivers' physiological information, the driving simulator for producing virtual traffic scenes, car running and driving environments, and for obtaining the drivers' operation behavior data, as well as a

breathalyzer tester for identifying the driver's BAC level. In addition, wine, purified water, and other materials were also needed in the experiments.

Figure 2 – Experimental apparatus

Experimental procedures

To exclude the influence of fatigue, drugs, and other impact factors, a time was selected to experiment in which the drivers were in good condition. Participants wearing the human factors experimental apparatus were required to conduct driving simulation experiments in normal driving state A (BAC=0), drinking-driving state B (BAC=0.03±0.01%), and drunk-driving state C (BAC=0.09±0.01%). All the data on participant physiology (heart rate, dermal electric), cars (velocity, acceleration), and the environment (lane shift, distance from leading car) was obtained. All drivers were organized to perform driving simulation experiments six times under every driving state. The valid data obtained in one experiment of every driver under every driving state was one data set, so 54·3·6=972 data sets were obtained, which included plenty of information on drivers' physiology, cars, and driving environments.

3D virtual driving scenes had been designed based on a driving simulator to provide realistic visual perception, auditory perception, and tactile sensation for the drivers. The driving scenes were from a common urban road environment, including straightaways, left and right curves with radiuses of 800 meters, 400 meters, and 200 meters, and crossroads. Traffic events including car-following and overtaking were set to motivate various driving operations. The design of the experimental road is shown in *Figure 3*.

3.2 Variable extractions

3.2.1 Variable selection

The influencing factors of drinking-driving recognition are various. With reference to correlational research [18-19], 18 common variables of driving behaviors had been selected, and the symbols and units of the variables are shown in *Table 1*.

The definitions of the variables are as follows:

$$J_m = \frac{1}{n}\sum_{i=1}^{n} J_i \tag{4}$$

$$H_m = \frac{1}{n}\sum_{i=1}^{n} H_i \tag{5}$$

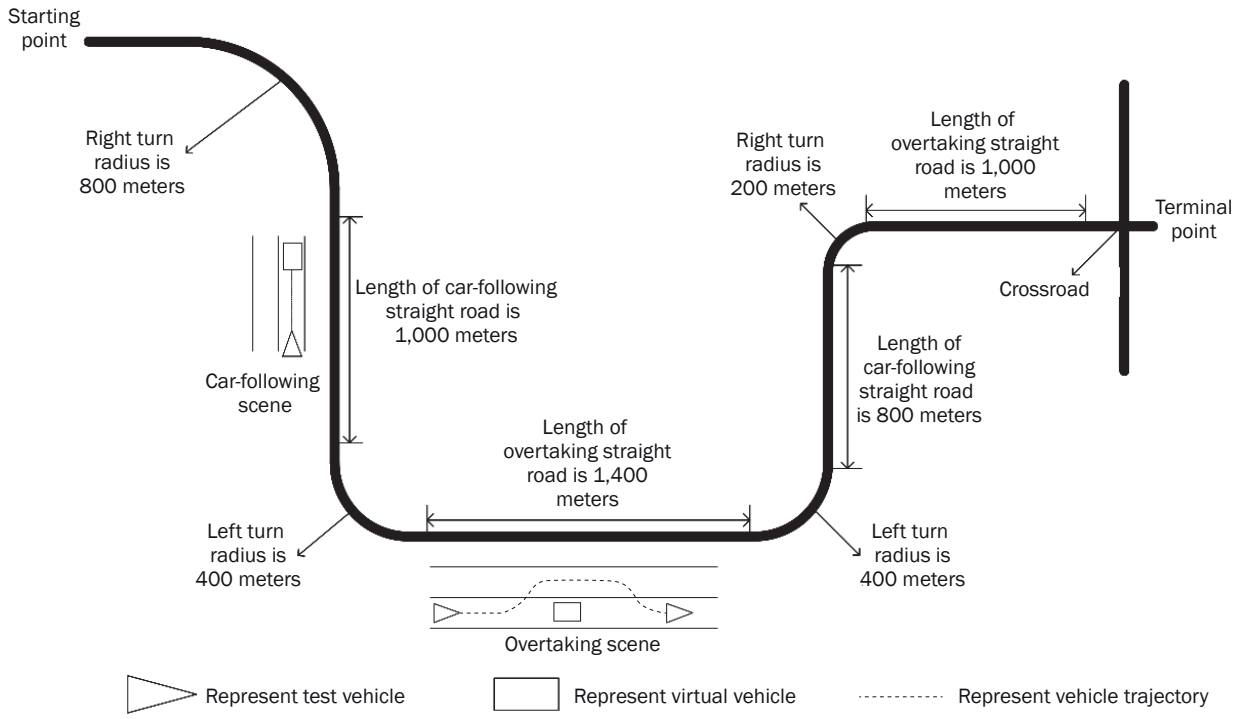

Figure 3 – The experimental road

Table 1 – Symbols and units of variables

Variable	Symbol	Units	Variable	Symbol	Units
Mean value of dermal electric	J_m	μΩ	Mean value of acceleration	A_m	m/s^2
Mean value of heart rate	H_m	bmp	Standard deviation of acceleration	A_S	m/s^2
Mean value of visual reaction time	T_m	s	Mean value of the front wheel angle	R_m	rad
Mean value of accelerator pedal pressure	F_{Um}	N	Standard deviation of the front wheel angle	R_S	rad
Standard deviation of accelerator pedal pressure	F_{US}	N	Mean value of distance from leading car	L_m	m
Mean value of brake pedal pressure	F_{Dm}	N	Standard deviation of distance from leading car	L_S	m
Standard deviation of brake pedal pressure	F_{DS}	N	Mean value of distance from the lane middle	B_m	m
Mean value of velocity	V_m	m/s	Standard deviation of distance from the lane middle	B_S	m
Standard deviation of velocity	V_S	m/s	Mean value of completing overtaking time	C_m	s

In the above formulas: the dermal electric and heart rate values are gathered at every second; J_i is the dermal electric value at the second i; H_i is heart rate value at the second i.

$$T_m = \frac{1}{n}\sum_{i=1}^{n} T_i \tag{6}$$

In the above formula: T_i is the visual reaction time value at the second i, which is from the driver receiving visual stimuli to making action response.

$$F_{Um} = \frac{1}{n}\sum_{i=1}^{n} F_{Ui} \tag{7}$$

$$F_{US} = \frac{1}{n}\sum_{i=1}^{n} (F_{Ui} - F_{Um})^2 \tag{8}$$

$$F_{Dm} = \frac{1}{n}\sum_{i=1}^{n} F_{Di} \tag{9}$$

$$F_{DS} = \frac{1}{n}\sum_{i=1}^{n} (F_{Di} - F_{Dm})^2 \tag{10}$$

In the above formulas: F_{Ui} is drivers' accelerator pedal pressure value at the second i; F_{Di} is drivers' brake pedal pressure value at the second i; the pedal pressure value is normalized from 0 to 1 (the pressure value is 0 when drivers do not tread the pedal, and the pressure value is 1 when drivers tread pedals to the maximum).

$$V_m = \frac{1}{n}\sum_{i=1}^{n} V_i \tag{11}$$

$$V_S = \frac{1}{n}\sum_{i=1}^{n} (V_i - V_m)^2 \tag{12}$$

In the above formulas: velocities of experimental cars are gathered at every second; V_i is velocity at the second i.

$$A_m = \frac{1}{n}\sum_{i=1}^{n} A_i \tag{13}$$

$$A_S = \frac{1}{n}\sum_{i=1}^{n} (A_i - A_m)^2 \tag{14}$$

In the above formulas: A_i is the acceleration value at the second i.

$$R_m = \frac{1}{n}\sum_{i=1}^{n} R_i \tag{15}$$

$$R_S = \frac{1}{n}\sum_{i=1}^{n} (R_i - R_m)^2 \tag{16}$$

In the above formulas: R_i is the front wheel angle at the second i; R_i is 0 when the steering wheel is straightened; R_i is negative when the steering wheel is turned left; R_i is positive when the steering wheel is turned right; drivers' steering wheel operation characteristics can be reflected by the front wheel angle.

$$L_m = \frac{1}{n}\sum_{i=1}^{n} L_i \tag{17}$$

$$L_S = \frac{1}{n}\sum_{i=1}^{n} (L_i - L_m)^2 \tag{18}$$

$$B_m = \frac{1}{n}\sum_{i=1}^{n} B_i \tag{19}$$

$$B_S = \frac{1}{n}\sum_{i=1}^{n} (B_i - B_m)^2 \tag{20}$$

In the above formulas: L_i is distance from the leading car to the second one in car-following scenes – the distance was measured from the front bumper of the experimental car to the tail bumper of the contiguous leading car; B_i is experimental car's distance from the lane middle at the second i – the experimental car's distance from the lane middle was measured from the right edge of the experimental car to the lane middle;

B_i is negative when the experimental car's right edge is on the left side of the lane middle; B_i is positive when the experimental car's right edge is on the right side of the lane middle.

$$C_m = \frac{1}{n}\sum_{i=1}^{n} C_i \quad (21)$$

In the above formula: C_i is the overtaking completion time at the second i. The overtaking completion time was kept from the moment the experimental car began to accelerate to its return to the original lane.

According to a correlation analysis, the above 18 variables were related to the driving state, and there were correlations between them. Therefore, their dimensions could be reduced by PCA to extract the principal components as the input vector of the RBF neural network which included major information on driving behaviors. The experimental data of driving behavior variables are partly shown in *Table 2*.

3.3 PCA

SPSS was used to carry out the PCA for the 18 variables. KMO (Kaiser-Meyer-Olkin) was 0.61>0.5; the Bartlett spherical test rejected the original hypothesis of the unit correlation matrix, P<0.001, and the PCA conditions were met. The sample data of the 18 initial variables were normalized and analyzed by PCA. The scree plot is shown in *Figure 4*.

In the above figure, the eigenvalues of the first seven components were higher, and the eigenvalues of the components behind the seventh component were smaller, so that the first seven components were selected as the principal components based on the inflection points of the curve and eigenvalues.

The variance explanations and the cumulative contribution rates of the principal components are shown in *Table 3*.

Table 2 – Partial experimental data of driving behavior variables

Time [s]	Car label	Mileage [m]	Distance from the lane middle [m]	Velocity [km/h]	Front wheel angle [rad]	Brake pedal pressure [n]	Accelerator pedal pressure [n]
1	1	761.61	1.71	4.77	0	0.31	0.19
1	2	797.12	1.50				
1	3	790.13	1.50				
2	1	766.05	1.68	4.45	0	0	0.66
2	2	800.14	1.50				
2	3	792.23	1.50				
3	1	772.47	1.63	6.43	0	0	1
3	2	803.16	1.50				
3	3	794.33	1.50				

Notes: there were three cars in the virtual driving scenes, car labeled 1 represented the experimental car that was operated by participants, cars labeled 2 and 3 represented virtual cars controlled by computers, and virtual cars were at a fixed speed. The driving simulator collected data at every second, and the experimental data of this table was captured over 3 seconds.

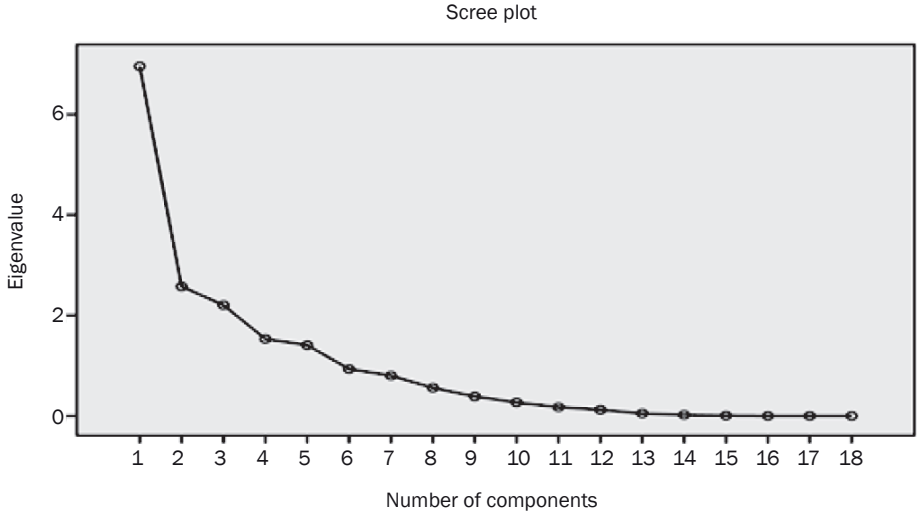

Figure 4 – Scree plot of each ingredient

Table 3 – The total variance explanations of the principal components

Principal component	Contribution rate [%]	Cumulative contribution rate [%]	Principal component	Contribution rate [%]	Cumulative contribution rate [%]
Z_1	38.64	38.64	Z_5	7.82	81.53
Z_2	14.31	52.95	Z_6	5.18	86.71
Z_3	12.25	65.20	Z_7	4.46	91.16
Z_4	8.51	73.71			

Table 4 – Score coefficients matrix of principle components

	Components						
	Z_1	Z_2	Z_3	Z_4	Z_5	Z_6	Z_7
λ_1	0.138	-0.011	0.026	-0.013	-0.091	0.094	-0.152
λ_2	0.122	0.110	0.102	0.012	-0.051	0.086	-0.285
λ_3	0.135	0.054	0.018	0.095	-0.065	0.042	0.016
λ_4	0.134	0.048	-0.017	0.011	-0.195	0.107	0.034
λ_5	-0.026	0.341	-0.059	-0.071	0.118	0.171	-0.178
λ_6	-0.101	-0.005	0.059	0.134	-0.033	0.601	0.173
λ_7	-0.009	0.122	0.259	-0.379	-0.109	-0.109	0.395
λ_8	-0.049	0.003	0.289	-0.069	0.386	0.159	-0.327
λ_9	0.053	0.061	0.097	0.105	0.456	-0.517	-0.012
λ_{10}	0.139	0.051	0.011	-0.006	0.039	0.100	-0.083
λ_{11}	0.070	-0.258	-0.003	-0.213	0.230	-0.078	0.145
λ_{12}	0.011	-0.328	0.041	-0.186	-0.101	0.034	0.016
λ_{13}	0.009	0.098	0.186	0.367	-0.058	-0.179	0.690
λ_{14}	-0.137	-0.040	-0.034	0.063	0.120	0.035	0.049
λ_{15}	0.055	-0.119	-0.294	0.297	0.169	0.010	0.105
λ_{16}	0.082	-0.003	-0.014	0.005	0.383	0.519	0.302
λ_{17}	-0.039	-0.102	0.227	0.377	-0.122	-0.051	-0.452
λ_{18}	-0.055	0.153	-0.315	-0.114	0.035	-0.159	-0.057

According to *Table 3*, the cumulative contribution rates of the first seven principal components reached 91.16%, including major information of the original variables. Therefore, these seven principal components were chosen to compose the input vector of the RBF neural network. The formula of the principal components is as follows:

$$\begin{aligned} z_i = {} & \lambda_{1i}J_m + \lambda_{2i}H_m + \lambda_{3i}T_m + \lambda_{4i}F_{Um} + \lambda_{5i}F_{US} + \lambda_{6i}F_{Dm} + \\ & + \lambda_{7i}F_{DS} + \lambda_{8i}V_m + \lambda_{9i}V_S + \lambda_{10i}A_m + \lambda_{11i}A_S + \lambda_{12i}R_m + \\ & + \lambda_{13i}R_S + \lambda_{14i}L_m + \lambda_{15i}L_S + \lambda_{16i}A_m + \lambda_{17i}B_S + \lambda_{18i}C_m \end{aligned} \quad (22)$$

In the above formula: z_i represents the principle component $i(i = 1,2,...,7)$.

The score coefficients matrix of the principle components on each original parameter is shown in *Table 4*. The seven principle components' data could be determined as the input sample data of the RBF neural network using the principal component formula and the original variables' data.

4. MODEL TRAINING AND RECOGNITION RESULT ANALYSIS

4.1 Model training

The algorithm code was programmed in Matlab. The 972 experimental data groups were analyzed by PCA, and then 922 experimental data groups were extracted randomly as the training sample data. The training sample data was imported after normalization into the RBF neural network to train the neural network. The remaining 50 experimental data groups were imported as the test sample data into the RBF neural network model which was trained completely; the output driving state values of the model were compared with expected driving state values to verify the model accuracy. The process of model training and validation is shown in *Figure 5*.

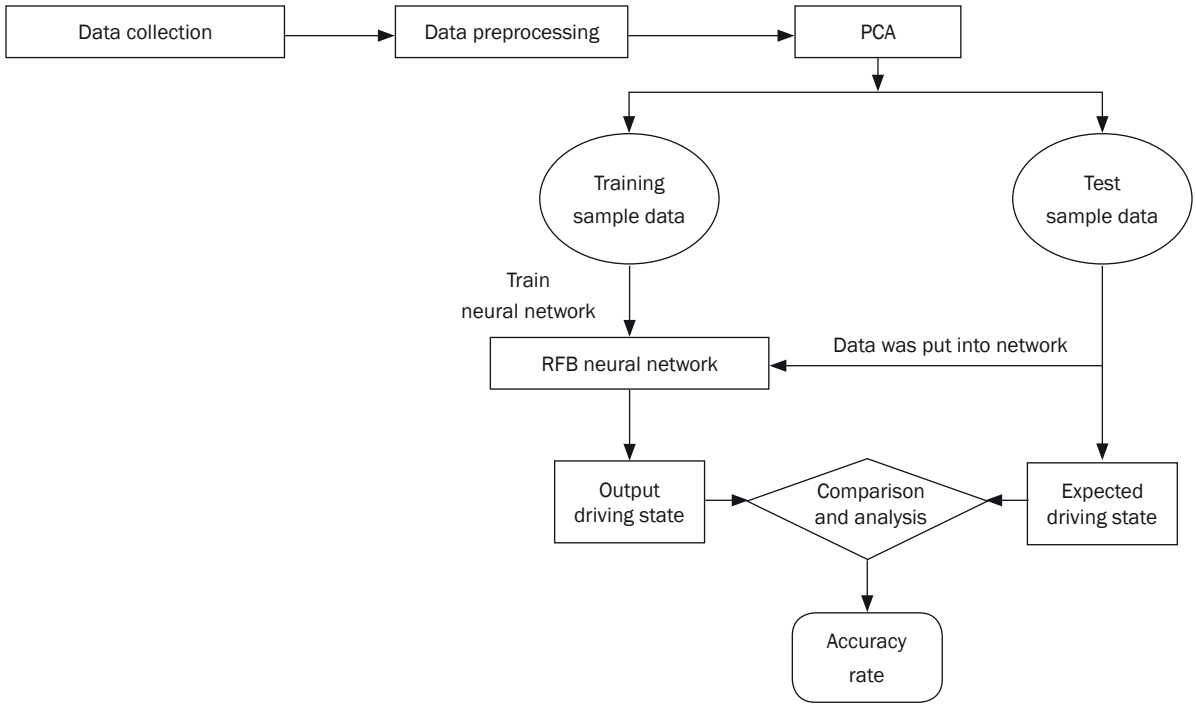

Figure 5 – Process of model training and validation

To obtain better network output, the network was trained and the parameters were optimized by an LM algorithm. The LM algorithm is a nonlinear optimization method which fuses the Newton method and gradient descent method. This algorithm has the capability of local convergence and global searching and uses approximate second derivative to improve the speed of network training. The parameter optimizing method of the LM algorithm [20] is as follows:

$$\begin{cases} h^{k+1} = h^k + \Delta h \\ \Delta h = -[J^T(h)J(h) + \mu I]^{-1} J(h)\delta(h) \end{cases} \quad (23)$$

In the above formula: h^k, h^{k+1} respectively represent the vectors composed by the weight values for the times k and k+1; Δh is the weight value increment. $J(h)$ is Jacobian matrix; $J^T(h)J(h)$ is Hessian matrix; I is unit matrix. μ(0<μ<1) is learning rate; if μ is higher, the LM algorithm is similar to the gradient descent method; if μ=0, the LM algorithm is the Newton method. During the optimization procedure, μ is a dynamic parameter. If a given μ can reduce the error, μ will decrease, otherwise it will increase.

4.2 Analyses of model recognition results

The evaluation indicator of model recognition errors (Δ) was mean square error (MSE), and the recognition accuracy of the model could be obtained based on MSE. The MSE formula is as follows:

$$MSE = \frac{\sum_{i=1}^{N} (|Y'| - |Y|)^2}{N} \quad (24)$$

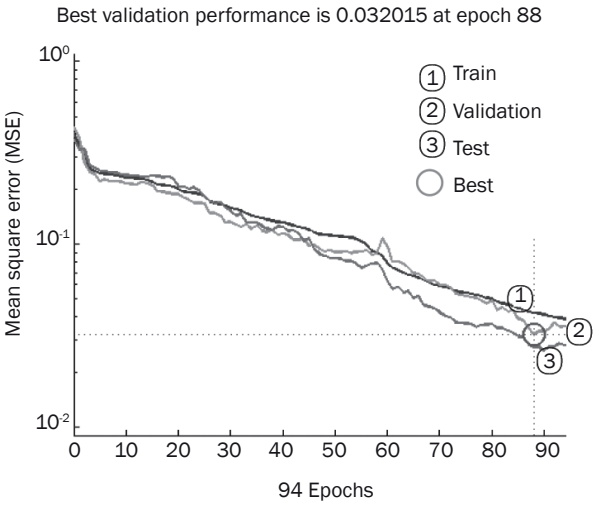

Figure 6 – Recognition error of RBF neural network

In the above formula: $|Y'| = |y_i|(i = 1,2,3)$ is the modulus of expected driving state vector; $|Y| = |y_i|(i = 1,2,3)$ is the modulus of model output driving state vector; N is the total number of test sample data groups.

The MSEs of the RBF neural network's training, validation, and testing are shown in *Figure 6*. According to *Figure 6*, there were 94 cycles of network training; the best MSE of validation was 0.032 at the eighty-eighth cycle; the model recognition error was small.

Through calculation, the training time of RBF neural network was 1.17 seconds, the speed of model calculation was relatively higher; the recognition accuracy

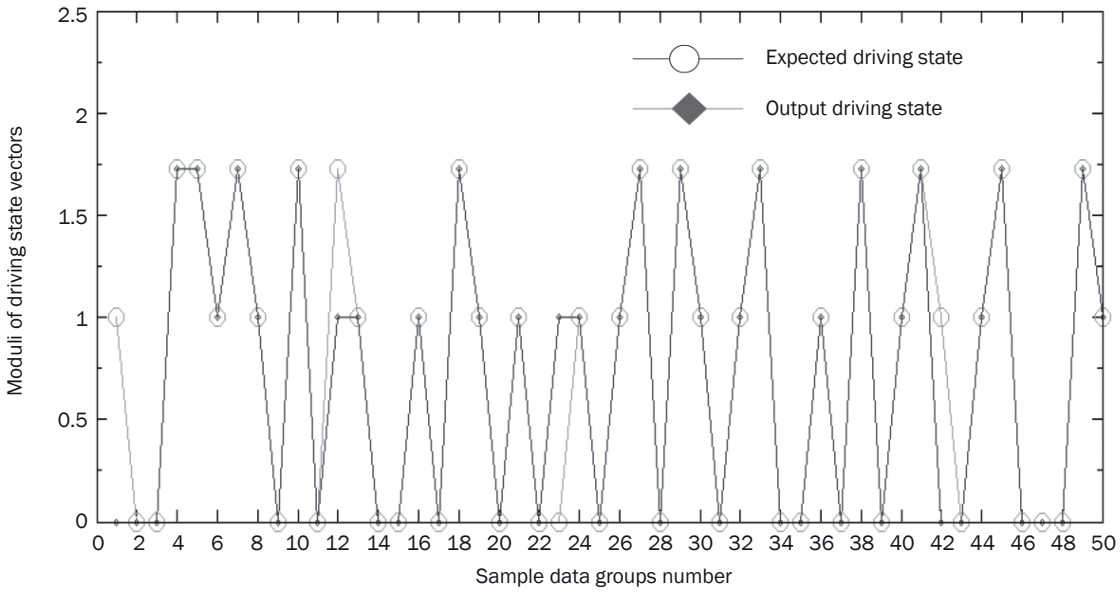

Figure 7 – Comparison of model output driving state vectors with expected driving state vectors
Notes: the vertical axis represents the moduli of driving state vectors; $|y_1|=|(1,1,1)|=\sqrt{3}\approx 1.73$ *represents normal driving state A;* $|y_2|=|(0,0,1)|=1$ *represents the drinking-driving state B ; represents the drunk driving state C (BAC=0.09±0.01%); the horizontal axis represents the 50 data groups.*

was 92.01%, which indicated the recognition accuracy of the model was high and the model could recognize whether the driver had been drinking or not.

After preprocessing, the 50 test sample data groups were imported into the trained RBF neural network model to obtain the model output driving state vector. To verify the accuracy of the drinking-driving recognition model based on PCA and the RBF neural network, the moduli of model output driving state vectors $|Y|=|y_i|(i=1,2,3)$ were compared to the moduli of expected driving state vectors $|Y'|=|y_i|(i=1,2,3)$. A comparison of model output driving state vectors with expected driving state vectors is shown in *Figure 7*.

In *Figure 7*, there were only four test sample data groups whose output driving state values did not meet expected driving state values. This means that the model output driving states were closely related to the expected driving states, and the fitting degree of the model was good.

Based on *Figure 6*, a consequence could be observed that the best MSE of the validation was 0.032, which indicates that there were small errors between the model output driving states and the actual driving states. In addition, according to *Figure 7*, most sample data could be recognized correctly by the proposed model, for there were only four data groups out of fifty getting the wrong outcomes. It can be concluded that the drinking-driving recognition model based on PCA and RBF neural network was able to accurately and efficiently identify whether the drivers had been drinking or not.

5. DISCUSSION

The drinking-driving recognition model was established based on the driving behavior data of drivers. The original variables were analyzed by PCA, and seven principal components were obtained. The principal components were the characteristic parameters of drinking-driving behaviors, which were used as the input vector to train the RBF neural network and build the drinking-driving recognition model. This way, the drinking-driving behaviors could be recognized and prevented during the driving process.

The influencing parameters in past studies had not been very adequate, leading to less than comprehensive analyses. The model in this paper could improve recognition accuracy by analyzing the drivers' physiological data, operation behavior data, car running data, and driving environment data comprehensively. The variables which influenced the recognition of drinking-driving behaviors the most were studied further. The driving behavior parameters' differences among drivers with different BAC levels were studied through variance analysis. According to the results, four variables of drivers with different BAC levels showed significant differences: the mean value of accelerator pedal pressure ($F(2,51)=8.784$, $p<0.05$), the mean value of velocity ($F(2,51)=7.614$, $p<0.05$), the standard deviation of acceleration ($F(2,51)=8.153$, $p<0.05$), and standard deviation of the front wheel angle ($F(2,51)=5.452$, $p<0.05$). The results of the variance analysis indicated that these four variables influenced the recognition of drinking-driving behaviors the most.

The model established in this paper can recognize drinking drivers automatically by using driving behavior data, which can be implemented in a car as part of advanced driver assistant systems. Driving behavior information can be gathered by installing the corresponding sensors in cars, and the information can be transmitted to the drinking-driving recognition model of the central control unit in real time. According to driving behavior data, the drinking-driving recognition model can determine whether the driver has been drinking or not. If the model determines that the driver is in a drinking-driving state, the central control unit will send the control instructions to the car, and the car will generate some responses, such as alarm, deceleration, acceleration ban, and so on. Thus we can stop drinking and driving on time, and maintain road traffic safety.

6. CONCLUSION

This study intends to establish a recognition model of drinking-driving behaviors, which can recognize drinking drivers accurately and efficiently during the driving process. The main conclusions of this paper are given as follows:

1) Complicated original variables were analyzed with PCA, and a few characteristic parameters containing the most of the driving information were extracted by PCA. The characteristic parameters were chosen as the input vector of the RBF neural network to reduce the amount of input data and improve RBF neural network efficiency.
2) The drinking-driving recognition model based on the RBF neural network was able to deal with complicated and dynamic driving behavior information. The model recognition accuracy reached 92.01%, and the best MSE of the validation was 0.032, which showed that the model had a good recognition performance.
3) There are also some limitations in our study. We have not considered other factors which may influence drinking-driving recognition, such as driving propensity, car type, road conditions, and so on. The sample data used to train the RBF neural network is not enough, and the recognition accuracy needs to be improved. In the future, to improve the accuracy of the drinking-driving recognition model, more factors will be incorporated into the model roundly, with additional sample data. To improve operation efficiency and stability of the network, the structure of the RBF neural network will be further optimized and a more advanced network training algorithm will be used. Through the above improvements, a more accurate and stabilized drinking-driving recognition model will be implemented into car driver assistant systems to manage drinking and driving effectively and maintain safety.

ACKNOWLEDGEMENT

This study was supported by the National Natural Science Foundation of China (Grant NO, 61573009), Natural Science Foundation of Shandong Province (Grant NO. ZR2017LF015), Project of Shandong Province Higher Educational Science and Technology Program (Grant NO. J15LB07).

孙一帆
山东理工大学 交通与车辆工程学院，淄博市，山东省，中国
电子邮箱：m18705423520@163.com
张敬磊，副教授（通讯作者）
山东理工大学 交通与车辆工程学院，淄博市，山东省，中国
电子邮箱：jinglei@sdut.edu.cn
王晓原，教授，博士
山东理工大学 交通与车辆工程学院，淄博市，山东省，中国
电子邮箱：2674289091@qq.com
王战古
山东理工大学 交通与车辆工程学院，淄博市，山东省，中国
电子邮箱: 1348035225@qq.com
于杰
山东理工大学 交通与车辆工程学院，淄博市，山东省，中国
电子邮箱:1206674681@qq.com

基于***PCA***与***RBF***神经网络的酒驾行为识别方法

摘要

酒驾行为是造成道路交通伤害的重要原因，严重威胁交通参与者的生命财产安全，因此，减少酒驾行为的发生成为交通安全研究的重要问题。选取能饮用适量酒精的*48*位男性驾驶员和*6*位女性驾驶员作为实验参与者。通过设计各种虚拟交通场景，组织驾驶员进行驾驶模拟实验，采集驾驶员的生理、操作行为、车辆运行及行驶环境数据。采用主成分分析*(PCA)*处理原始变量，将获得的*7*个主成分作为径向基函数*(RBF)*神经网络的输入向量，利用主成分的数据来训练和验证*RBF*神经网络。选择*LM*（*Levenberg-Marquardt*）算法训练网络参数，构建基于*PCA*和*RBF*神经网络的酒驾识别模型，实现对酒后驾驶行为的准确识别。测试结果表明，基于*PCA*和*RBF*神经网络的酒驾识别模型能在驾驶过程中准确识别饮酒驾驶员，识别准确率为*92.01%*，模型的运算效率较高。该研究可为防治酒后驾驶，维护交通安全提供了有益借鉴。

关键词：

交通安全；酒后驾驶行为；识别方法；主成分分析；径向基函数神经网络

REFERENCES

[1] Olmuş H, Erbaş S. Analysis of Traffic Accidents Caused by Drivers by Using Log-Linear Models. *Promet – Traffic & Transportation*. 2012;24(6): 495-504.
[2] Sheng-Cai LI, Xiao L. Statistics of industrial accidents in China during the period from January to February in 2016. *Journal of Safety & Environment*; 2016.

[3] González-Iglesias B, Gómez-Fraguela JA, Sobral J. Potential Determinants of Drink Driving in Young Adults. *Traffic Injury Prevention*. 2015;16(4).

[4] McCartt AT, Wells JK, Teoh ER. Attitudes toward in-car advanced alcohol detection technology. *Traffic Injury Prevention.* 2010;11(11): 156-164.

[5] Wu YC, Xia YQ, Xie P, et al. The Design of an Automotive Anti-Drunk Driving System to Guarantee the Uniqueness of Driver. *International Conference on Information Engineering and Computer Science IEEE*. 2009: 1-4.

[6] Li Z, Han J, Zhao X, et al. Comparison of Drunk Driving Recognizing Methods Based on KNN and SVM. *Journal of transportation systems engineering and information technology.* 2015;15(5): 246-251.

[7] Li YC, Sze NN, Wong SC, et al. A simulation study of the effects of alcohol on driving performance in a Chinese population. *Accident Analysis and Prevention.* 2016;95: 334-342.

[8] Zhao X, Zhang X, Rong J. Study of the Effects of Alcohol on Drivers and Driving Performance on Straight Road. *Mathematical Problems in Engineering.* 2014;2014(1): 1-9.

[9] Xu L, Qian F, Li Y, et al. Resource allocation based on quantum particle swarm optimization and RBF neural network for overlay cognitive OFDM System. *Neurocomputing*. 2016;173(P3): 1250-1256.

[10] Centeno LLR, Müller C, Ribeiro SM. Cognitive radio signal classification based on subspace decomposition and RBF neural networks. *Wireless Networks*. 2016;24(3): 1-11.

[11] Csekő LH, Kvasnica M, Lantos B. Explicit MPC-Based RBF Neural Network Controller Design with Discrete-Time Actual Kalman Filter for Semiactive Suspension. *IEEE Transactions on Control Systems Technology*. 2015;23(5): 1736-1753.

[12] Song E, Kim J, Lee S. Geometric Surface Reconstruction via LM Optimization algorithm. *Journal of Clinical Investigation.* 2015;63(3): 388-394.

[13] Zhou F, Zhu X. Earthquake Prediction Based on LM-BP Neural Network. *Lecture Notes in Electrical Engineering.* 2014;270: 13-20.

[14] Nguyen-Truong HT, Le HM. An implementation of the Levenberg-Marquardt algorithm for simultaneous-energy-gradient fitting using two-layer feed-forward neural networks. *Chemical Physics Letters*. 2015;629(1): 40-45.

[15] Li BN, Yu Q, Wang R, et al. Block PCA With Nongreedy ℓ_1-Norm Maximization. *IEEE Transactions on Cybernetics;* 2015.

[16] Skrobot VL, Castro EVR, Pereira RCC, et al. Use of Principal Component Analysis (PCA) and Linear Discriminant Analysis (LDA) in Gas Chromatographic (GC) Data in the Investigation of Gasoline Adulteration. *Energy & Fuels*. 2007;21(6): 5-19.

[17] Rao KD, Laxminarayana P, Reddy KC. RBF Neural Networks for Transient Identification in Nuclear Power Plants. *IETE Journal of Research*. 1997;43(6): 449-452.

[18] Zhang X, Zhao X, Du H, et al. Effect of different breath alcohol concentrations on driving performance in horizontal curves. *Accident Analysis & Prevention*. 2014;72: 401-10.

[19] Zhang XJ, Zhao XH, Jian R, et al. Study on the Individual Characteristics and Differences of Driving Behavior in Curves. *Journal of Highway & Transportation Research & Development*. 2015;9(1): 99-104.

[20] Fusco R, Sansone M, Petrillo A. The Use of the Levenberg–Marquardt and Variable Projection Curve-Fitting Algorithm in Intravoxel Incoherent Motion Method for DW-MRI Data Analysis. *Applied Magnetic Resonance*. 2015;46(5): 551-558.